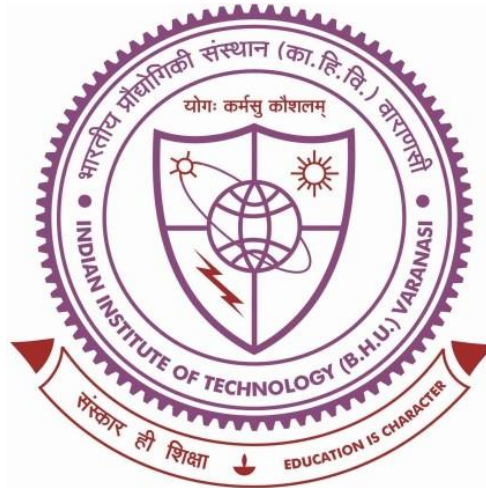


STUDIES ON TRIBOLOGICAL BEHAVIOUR OF Ni_3Al BASED SELF LUBRICATING COMPOSITES



Thesis submitted in partial fulfillment for the
Award of Degree

Doctor of Philosophy

By

Nitish Kumar Mahto

DEPARTMENT OF MECHANICAL
ENGINEERING INDIAN INSTITUTE OF
TECHNOLOGY (BANARAS HINDU
UNIVERSITY)
VARANASI - 221005
INDIA

Roll No. 18131010

2023

CERTIFICATE

It is certified that the work contained in the thesis titled "*STUDIES ON TRIBOLOGICAL BEHAVIOUR OF Ni₃Al BASED SELF LUBRICATING COMPOSITES*" by "*NITISH KUMAR MAHTO*" has been carried out under our supervision and that this work has not been submitted elsewhere for a degree.

It is further certified that the student has fulfilled all the requirements of Comprehensive Examination, Candidacy, and SOTA for the award of Ph.D. Degree.



Supervisor
(Prof. Sanjay Kumar Sinha)
IIT (BHU), Varanasi
INDIA



Co-Supervisor
(Prof. Rajnesh Tyagi)
IIT (BHU), Varanasi
INDIA

DECLARATION BY THE CANDIDATE

I, "**Nitish Kumar Mahto**", certify that the work embodied in this thesis is my own bonafide work and carried out by me under the supervision of "**Prof. Sanjay Kumar Sinha and Prof. Rajnesh Tyagi**" from "**July 2018**" to "**December 2023**", at the "**Department of Mechanical Engineering**", Indian Institute of Technology (BHU), Varanasi, India. The matter embodied in this thesis has not been submitted for the award of any other degree/diploma.

I declare that I have faithfully acknowledged and given credits to the research workers wherever their works have been cited in my work in this thesis. I further declare that I have not wilfully copied any other's work, paragraphs, text, data, results, *etc.*, reported in journals, books, magazines, reports, dissertations, theses, *etc.*, or available at websites and have not included them in this thesis and have not cited as my own work.

Date: 12.12.2023

Place: IIT BHU Varanasi

Nitish Kumar Mahto
(NITISH KUMAR MAHTO)

CERTIFICATE BY THE SUPERVISORS

It is certified that the above statement made by the student is correct to the best of our knowledge.



Supervisor

(Prof. Sanjay Kumar Sinha)

IIT (BHU), Varanasi

INDIA

प्राध्यापक / Professor

यांत्रिक अभियान्त्रिकी विभाग/Deptt. of Mechanical Engg.

भारतीय प्रौद्योगिकी संस्थान / Indian Institute of Technology

(का०हि०वि०/B.H.U.)

वाराणसी-221005 / Varanasi-221005

Signature of Head of Department

[Signature]
विभागाध्यक्ष / HEAD

यांत्रिक अभियान्त्रिकी विभाग/Deptt. of Mechanical Engg.

भारतीय प्रौद्योगिकी संस्थान / Indian Institute of Technology

(का०हि०वि०/B.H.U.)

वाराणसी-221005 / Varanasi-221005



Co-Supervisor

(Prof. Rajnesh Tyagi)

IIT (BHU), Varanasi

INDIA

प्राध्यापक / Professor

यांत्रिक अभियान्त्रिकी विभाग/Deptt. of Mechanical Engg.

भारतीय प्रौद्योगिकी संस्थान / Indian Institute of Technology

(का०हि०वि०/B.H.U.)

वाराणसी-221005 / Varanasi-221005

iii | Page

COPYRIGHT TRANSFER CERTIFICATE

Title of the Thesis: *Studies on tribological behaviour of Ni₃Al based self-lubricating Composites*

Name of the Student: NITISH KUMAR MAHTO

Copyright Transfer

The undersigned hereby assigns to the Indian Institute of Technology (Banaras Hindu University), Varanasi, all rights under copyright that may exist in and for the above thesis submitted for the award of the **Doctor of Philosophy**.

Date: 12.12.2023

Place: IIT BHU Varanasi

Nitish Kumar Mahto
(Nitish Kumar Mahto)

Note: However, the author may reproduce or authorize others to reproduce material extracted verbatim from the thesis or derivative of the thesis for the author's personal use, provided that the source and the Institute's copyright notice are indicated.

ACKNOWLEDGEMENT

The author is pleased to express his sincere thanks and gratitude beyond words to his supervisor Prof. Sanjay Kumar Sinha and co-supervisor Prof. Rajnesh Tyagi for their consistent help, encouragement and valuable discussions during the entire period of his research work. The author would not have been able to complete the thesis without their utmost involvement and invaluable efforts. They motivated the author to pursue research problems and the need for persistent effort to accomplish the goal. The author is truly indebted to them.

Besides supervisors, the author would like to thank his RPEC members, Prof. Uppu Srinivas Rao and Prof. Vikas Jindal for their insightful comments and encouragement. The author acknowledges his deep sense of gratitude to the current and former Heads of the Department of Mechanical Engineering for providing all the research facilities to accomplish his research in the Department successfully. The author has an immense sense of gratitude to all the faculty members of the Department of Mechanical Engineering, IIT (BHU), Varanasi for their cooperation and inspiration.

The author is thankful to the unknown reviewers who have rejected my papers several times in journals. The comments that they provided helped polish our articles and put them in better shape. Nevertheless, the bigger and nobler cause of thanking them is that the rejections have equipped me with a high level of patience and helped me to implement my spiritual thoughts in practice. My acknowledgement will never be complete without the special mention to my lab seniors and colleagues for their great help during five years of the Ph.D. journey- Dr. Rohit Kumar Singh Gautam, Dr. Manish Kumar, Dr. Hemant Nautiyal, Dr. Sudesh Singh, Dr. Ashwani Ranjan, Dr. Pooja Verma, Km Shafali, Mr. Ashwani Sharma, Mr. Hemant Kumar, Mr. Abhimanyu Chaudhari, Mrs. Smita Gupta and

Mr. Abhay Kumar. I convey my gratitude to all my teachers throughout my academic career for preparing me to walk through this long journey. The author is also thankful to all the lab, workshop, CIFIC, and office staff of the department, especially Mr. Vijay Pratap Srivastava (CAM lab) and Aman, Sachin and Sudhakar (CIFIC lab). I want to thank the administrative personnel at IIT BHU for helping me with their expertise during several requirements that had to be met over the entire course of the Ph.D. at IIT BHU.

Last but not least, words fail me to express my appreciation when it is time to share my gratitude to those very special people who always stood like a pillar of strength, my grand-mother Smt. Chutni Devi, my parents Shri Shiva Prasad Mahto and Smt. Shobha Devi, wife Sujeeta Biswas, uncle Shri Hari Prasad Mahto, Aunt Smt. Padmini Devi and brother Goutam Kumar Mahto.

At last, regards to the almighty God who has given the author spiritual support and courage to carry out this work.

(NITISH KUMAR MAHTO)

List of Figures

Fig. 2.1:	Matrix based classification of composites.	8
Fig. 2.2:	Classification of the processing routes to develop MMCs.	9
Fig. 2.3:	Steps involved in powder metallurgy process.	11
Fig. 2.4:	A schematic diagram of sintering.	12
Fig. 2.5:	Typical solid lubricants	24
Fig. 2.6:	The applicable working temperature range for different self-lubricating materials	26
Fig. 3.1:	Process flow for synthesis of Cu-modified hBN (Cu-hBN) nanosheets.	49
Fig. 3.2:	Schematic diagram of a typical vacuum hot press sintering furnace.	51
Fig. 3.3:	Schematic diagram of high-temperature ball-on-disc tribometer set up for friction and wear tests.	55
Fig. 4.1:	FESEM micrographs of elemental powders: (a) Ni, (b) Mo, (c) Al, (d) Cr, (e) Zr, (f) B, (g) WS ₂ , (h) Ag, and their XRD analyses (i) and (j).	61
Fig. 4.2:	FESEM micrographs of milled powders: (a) Ni ₃ Al, (b) Ni ₃ Al-10Ag, (c) Ni ₃ Al-10WS ₂ , and (d) Ni ₃ Al-5Ag-5WS ₂ , and their thermo-gravimetric analysis (e).	63
Fig. 4.3:	X-ray diffraction patterns of (a) ball milled powder and (b) vacuum hot pressed sintered composite for Ni ₃ Al, Ni ₃ Al-10Ag, Ni ₃ Al-10WS ₂ , and Ni ₃ Al-5Ag-5WS ₂ .	63
Fig. 4.4:	Microstructures of (a) Ni ₃ Al, (b) Ni ₃ Al-10Ag, (c) Ni ₃ Al-10WS ₂ , and (d) Ni ₃ Al-5Ag-5WS ₂ and corresponding EDS elemental mapping.	65

- Fig. 4.5:** Microhardness (HV) indentation images of (a) Ni₃Al, (b) Ni₃Al-10Ag, (c) Ni₃Al-10WS₂, and (d) Ni₃Al-5Ag-5WS₂. 66
- Fig. 4.6:** Variation of coefficient of friction with time at (a) RT, (b) 200 °C, (c) 400 °C, (d) 600 °C and (e) 800 °C for the Ni₃Al, Ni₃Al-10Ag, Ni₃Al-10WS₂ and Ni₃Al-5Ag-5WS₂ composite. 68
- Fig. 4.7:** Variation of average coefficient of friction with temperature for the Ni₃Al, Ni₃Al-10Ag, Ni₃Al-10WS₂ and Ni₃Al-5Ag-5WS₂ composite. 69
- Fig. 4.8:** Variation of wear rates with temperature for the Ni₃Al, Ni₃Al-10Ag, Ni₃Al-10WS₂ and Ni₃Al-5Ag-5WS₂ composite. 70
- Fig. 4.9:** FESEM micrographs of the worn-out Ni₃Al composite at (a) RT (b) 200 °C (c) 400 °C (d) 600 °C (f) 800 °C, and EDS analysis of worn NI at 600 °C and 800 °C (e and g). 72
- Fig. 4.10:** FESEM micrographs of the worn-out silicon nitride ball (counterface) (a) RT (b) 200 °C (c) 400 °C (d) 600 °C (f) 800 °C, and EDS analysis of worn Si₃N₄ ball at 600 °C and 800 °C (e and g). 73
- Fig. 4.11:** FESEM micrographs of the worn-out Ni₃Al-10Ag composite at (a) RT (b) 200 °C (c) 400 °C (d) 600 °C (e) 800 °C, and EDS analysis of worn NI-10A at 400 °C and 600 °C (f and g) as well as area elemental mapping of Ni, O, Ag and Mo at 800 °C (h). 75
- Fig. 4.12:** FESEM micrographs of the worn-out silicon nitride ball (counterface) (a) RT (b) 200 °C (c) 400 °C (d) 600 °C (e) 800 °C and its EDS analysis. 76
- Fig. 4.13:** FESEM micrographs of the worn-out Ni₃Al-10WS₂ composite at (a) RT (b) 200 °C (c) 400 °C (d) 600 °C (e) 800 °C and its EDS analysis. 77

- Fig. 4.14:** FESEM micrographs of the worn-out silicon nitride ball (counterface) (a) RT (b) 200 °C (c) 400 °C (d) 600 °C (e) 800 °C and its EDS analysis. 78
- Fig. 4.15:** FESEM micrographs of the worn-out Ni₃Al-5Ag-5WS₂ composite at (a) RT (b) 200 °C (c) 400 °C (d) 600 °C (e) 800 °C along with the corresponding area elemental mapping of Ni, Al, Cr, Mo, W, S, O and Ag. 79
- Fig. 4.16:** FESEM micrographs of the worn-out Si₃N₄ ball (counterface) (a) RT (b) 200 °C (c) 400 °C (d) 600 °C (e) 800 °C along with the corresponding area elemental mapping of Si, N, Al, S, Ni, Mo, Cr, W, O and Ag. 80
- Fig. 4.17:** X-ray diffraction patterns of worn composite (a) Ni₃Al, (b) Ni₃Al-10Ag, (c) Ni₃Al-10WS₂, and (d) Ni₃Al-5Ag-5WS₂ at various temperatures. 82
- Fig. 4.18:** Raman spectra of worn composite (a) Ni₃Al, (b) Ni₃Al-10Ag, (c) Ni₃Al-10WS₂, and (d) Ni₃Al-5Ag-5WS₂ at various temperatures. 83
- Fig. 4.19:** FESEM micrographs of cross-section or subsurface of worn track at 800 °C corresponding to (a) Ni₃Al, (b) Ni₃Al-10Ag, (c) Ni₃Al-10WS₂, and (d) Ni₃Al-5Ag-5WS₂ composites and microhardness of glaze layer on NI-10AW at 800 °C (e). 84
- Fig. 4.20:** Schematic illustration depicting the wear mechanism of NI, NI-10A, NI-10W and NI-10AW composites. 90
- Fig. 5.1:** TEM images of (a-c) *h*-BNNSs and (d-f) Cu-*h*BN at different magnifications along with corresponding area elemental (Boron, Nitrogen, and Copper) distribution. 95
- Fig. 5.2:** XRD pattern of Cu-*h*BN along with assignment of diffraction features. 96

- Fig. 5.3:** Wide scan spectrum of Cu-*h*BN along with high-resolution B 1s, C 1s, N 1s, O 1s, and Cu 2p XPS spectra. The high-resolution Cu 2p spectrum is deconvoluted to reveal different oxidation states of Cu in their oxides. 97
- Fig. 5.4:** FESEM images and corresponding elemental maps of ball-milled powders: (a) NI, (b) NI-10Ag, (c) NI-10BN, and (d) NI-10AgBN. 99
- Fig. 5.5:** XRD patterns of (a) ball-milled powders and (b) vacuum hot press sintered composite. 100
- Fig. 5.6:** FESEM micrographs showing the microstructure of (a) NI, (b) NI-10Ag, (c) NI-10BN and (d) NI-10AgBN and corresponding EDS elemental mapping. 102
- Fig. 5.7:** Fluctuation in coefficient of friction with time for Ni₃Al (NI) and composites, NI-10Ag, NI-10BN, and NI-10AgBN at (a) RT, (b) 200 °C, (c) 400 °C, (d) 600 °C and (e) 800 °C. 104
- Fig. 5.8:** Variation of average coefficient of friction with temperature for NI and its composites, i.e., NI-10Ag, NI-10BN, and NI-10AgBN. 105
- Fig. 5.9:** Variation of wear rate with temperature for NI and composites, NI-10Ag, NI-10BN and NI-10AgBN. 106
- Fig. 5.10:** FESEM images of the worn surface of NI composite at (a) RT (b) 200 °C (c) 400 °C (d) 600 °C (e) 800 °C and (f) elemental mapping of worn surface NI at 800 °C. 107
- Fig. 5.11:** FESEM images of the worn surface of counterface Si₃N₄ ball: (a) RT, (b) 200 °C, (c) 200 °C, (d) 600 °C, (e) 800 °C, and (f) EDS analysis of the ball at 800 °C. 108
- Fig. 5.12:** FESEM images of the worn surface of NI-10Ag composite at (a) RT (b) 200 °C (c) 400 °C (d) 600 °C (e) 800 °C and (f) elemental mapping of worn NI-10Ag at 800 °C. 110

- Fig. 5.13:** FESEM images of the worn surface of counterface Si₃N₄ ball: (a) RT, (b) 200 °C, (c) 200 °C, (d) 600 °C, (e) 800 °C, and (f) EDS analysis of the ball at 800 °C. 110
- Fig. 5.14:** FESEM images of the worn surface of NI-10BN composite at (a) RT (b) 200 °C (c) 400 °C (d) 600 °C (e) 800 °C and (f) elemental mapping of worn NI-10BN at 800 °C. 112
- Fig. 5.15:** FESEM images of the worn surface of counterface Si₃N₄ ball: (a) RT, (b) 200 °C, (c) 400 °C, (d) 600 °C, (e) 800 °C, and (f) EDS analysis of the ball at 800 °C. 113
- Fig. 5.16:** FESEM images of the worn surface of NI-10AgBN composite at (a) RT (b) 200 °C (c) 400 °C (d) 600 °C (e) 800 °C and (f) elemental mapping of worn NI-10BN at 800 °C. 115
- Fig. 5.17:** FESEM images of the worn surface of counterface Si₃N₄ ball: (a) RT, (b) 200 °C, (c) 200 °C, (d) 600 °C, (e) 800 °C, and (f) elemental mapping of worn ball at 800 °C. 116
- Fig. 5.18:** XRD patterns of worn specimens (a) NI, (b) NI-10Ag, (c) NI-10BN, and (d) NI-10AgBN at different temperatures. 117
- Fig. 5.19:** Raman spectra of worn specimens of (a) NI, (b) NI-10Ag, (c) NI-10BN, and (d) NI-10AgBN at various temperatures. 119
- Fig. 5.20:** FESEM micrographs (backscattered mode) and EDS analysis of cross-section of worn track at 800 °C corresponding to (a) NI, (b) NI-10Ag, (c and d) NI-10BN, and (e and f) NI-10AgBN composites. 121
- Fig. 5.21:** TEM images of (a-c) Cu-*h*BN at different magnifications and (d) area elemental mapping of Cu-*h*BN. 128
- Fig. 5.22:** XRD pattern of Cu doped *h*BN nanosheets. 130

- Fig. 5.23:** XPS spectra of Cu-doped *h*BN powders showing full scan survey (a) and corresponding de-convoluted peaks in the high-resolution spectra for (b) B 1s, (c) N 1s (d) C 1s (e) Cu 2P and (f) O 1s. 130
- Fig. 5.24:** Microscopic images of mechanically alloyed powders: (a) NA, (b) NAW, (c) NAB, and (d) NAWB and (e) elemental mapping of NAWB. 132
- Fig. 5.25:** HR-XRD patterns for NA, NAW, NAB, and NAWB (a) mechanically alloyed powders and (b) sintered composite. 132
- Fig. 5.26:** FESEM micrographs showing the microstructure of (a) NA, (b) NAW, (c) NAB and (d) NAWB and (e) elemental mapping of NAWB composite. 134
- Fig. 5.27:** Time-dependent friction profiles for NA, NAW, NAB, and NAWB at (a) RT, (b) 200 °C, (c) 400 °C, (d) 600 °C, and (e) 800 °C. 135
- Fig. 5.28:** Temperature-dependent graphical plots of coefficient of friction for NA, NAW, NAB, and NAWB. 136
- Fig. 5.29:** Temperature-dependent wear plots for NA, NAW, NAB, and NAWB. 137
- Fig. 5.30:** FESEM images of the worn surface of NA: (a) RT, (b) 200 °C, (c) 400 °C, (d) 600 °C, (f) 800 °C, and (e and g) EDS and elemental mapping of worn surface of NA at 600 °C and 800 °C. 139
- Fig. 5.31:** FESEM images of the worn surface of counterface Si₃N₄ ball: (a) RT, (b) 200 °C, (c) 400 °C, (d) 600 °C, (e) 800 °C, and (f) EDS analysis of transfer film on the ball at 800 °C. 139
- Fig. 5.32:** FESEM images of the worn surface of NAW: (a) RT, (b) 200 °C, (c) 400 °C, (d) 600 °C, (e) 800 °C, and (f and g) EDS analysis of worn surface of NAW at 600 °C and 800 °C. 141

- Fig. 5.33:** FESEM images of the worn surface of counterface Si₃N₄ ball: (a) RT, (b) 200 °C, (c) 400 °C, (d) 600 °C, (e) 800 °C, and (f) EDS analysis of transfer film on the ball at 800 °C. 142
- Fig. 5.34:** FESEM images of the worn scar of NAB composite at (a) RT, (b) 200 °C, (c) 400 °C, (d) 600 °C, (e) 800 °C, and (f, g and h) EDS and elemental maps of worn track at 600 °C and 800 °C. 144
- Fig. 5.35:** FESEM images of the worn scar of Si₃N₄ ball at (a) RT, (b) 200 °C, (c) 400 °C, (d) 600 °C, (e) 800 °C, and (f) EDS analysis of transfer film on worn Si₃N₄ ball (counterface) at 800 °C. 145
- Fig. 5.36:** FESEM images of the worn scar of NAWB composite at (a) room temperature, (b) 200 °C, (c) 400 °C, (d) 600 °C, (e) 800 °C, and (f and g) EDS and elemental maps of worn track at 600° C and 800 °C. 147
- Fig. 5.37:** FESEM images of the worn scar of Si₃N₄ ball at (a) room temperature, (b) 200 °C, (c) 400 °C, (d) 600 °C, (e) 800 °C, and (f) elemental maps of transfer film on worn Si₃N₄ ball (counterface) at 800 °C. 148
- Fig. 5.38:** XRD patterns of worn composite specimens (a) NA, (b) NAW, (c) NAB, and (d) NAWB at various temperatures. 149
- Fig. 5.39:** Raman spectra of worn specimens of (a) NA, (b) NAW, (c) NAB, and (d) NAWB at various temperatures. 151
- Fig. 5.40:** Schematic illustration of lubrication and material removal from RT-200 °C, 200 °C-400 °C, and 600 °C -800 °C for (a) NA, (b) NAW, (c) NAB and (d) NAWB. 158
- Fig. 5.41:** Variation of (a) average coefficient of friction and (b) specific wear rate with temperature for Ni₃Al and its composites, i.e., Ni₃Al-10Ag (NI-10A), Ni₃Al-10WS₂ (NI-10W), Ni₃Al-10Cu-*h*BN (NI-10B), Ni₃Al-5Ag-5WS₂ (NI-10AW), Ni₃Al-5Ag-5Cu-*h*BN (NI-10AB) and Ni₃Al-5WS₂-5Cu-*h*BN (NI-10WB). 161

List of Tables

Table 2.1: Review on Ni-based high-temperature solid-lubricating coatings	29
Table 2.2: Review of the tribological properties of Ni-based high-temperature solid-lubricating composites	32
Table 2.3: Review of the tribological properties of intermetallic (Ni ₃ Al and NiAl) matrix solid-lubricating composites or coatings.	35
Table 3.1: Composition and vacuum hot press sintering parameters of Ni ₃ Al-based composites.	50
Table 3.2: Composition and vacuum hot press sintering parameters of Ni ₃ Al-based composites.	50
Table 3.3: Composition and vacuum hot press sintering parameters of Ni ₃ Al-based composites.	51
Table 3.4: Tribological testing parameters for Ni ₃ Al-based composites	56
Table 4.1: Specimen designation, composition, density, and microhardness.	66
Table 5.1: Sample designation, composition, density (real and relative), and microhardness.	98
Table 5.2: Sample notation, composition, density and micro-hardness.	131

List of abbreviations & symbols

Cu- <i>h</i> BN	:	Copper modified or doped <i>h</i> BN nanosheets
<i>d</i>	:	Interplanar spacing
2D	:	Two dimensional
EDS	:	Energy Dispersive X-ray spectroscopy
FE-SEM	:	Field Emission Scanning Electron Microscopy
<i>g</i>	:	Gram
hr.	:	Hour
HV	:	Vickers hardness
<i>k</i> Hz	:	Frequency
K	:	Kelvin
min	:	Minute
<i>mm</i> ³ / <i>Nm</i>	:	Wear rate
ml/min	:	Flow rate
<i>mL</i>	:	Milliliter
MPa	:	Mega Pascal
m/s	:	Sliding speed
<i>n</i>	:	Integer representing order of the diffraction
N	:	Normal load
<i>rpm</i>	:	Revolution per minute
RT	:	Room temperature
S	:	Sliding distance
SEM	:	Scanning electron microscopy
<i>s</i>	:	Second
TEM	:	Transmission electron microscope

V	:	Volume loss
VHPS	:	Vacuum hot press sintering
W	:	Wear volume loss
wt. %	:	Weight percentage
XPS	:	X- ray photoelectron spectroscopy
XRD	:	X- ray diffraction
°C	:	Degree Celsius
°C/min	:	Heating rate
%	:	Percentage
k	:	Wear coefficient
μm	:	Micrometer
μ	:	Coefficient of friction
λ	:	Wavelength of the x-ray
θ	:	Incident angle
γ	:	Delta